LOWLAND TECHNOLOGY INTERNATIONAL Vol. 3, No. 2, 15-30, December 2001
International Association of Lowland Technology (IALT), ISSN 1344-9656

ANALYTICAL MODEL OF HEXAGONAL WIRE MESH REINFORCEMENT WITH WEATHERED BANGKOK CLAY BACKFILL

D.T. Bergado [1], P. Voottipruex[2], A. Asanprakit[3] and C. Teerawattanasuk[4]

ABSTRACT: An analytical method is proposed for determining the pullout resistance/pullout displacement relationship for both of PVC-coated and zinc-coated hexagonal wire mesh reinforcement. The parameters used in this analytical model were obtained from pullout testing programs, such as shear stiffness (k_s) and initial slope of pullout bearing resistance (E_{ip}). In addition, this method can predict the movement characteristics of both PVC-coated and zinc-coated hexagonal mesh during pullout. The displacements along the reinforcement axial stiffness and the friction resistance can be simulated by linear, elastic-perfectly plastic model. The hyperbolic model can be used to calculate the bearing resistance. Reasonable agreement between the predicted and measured pullout resistances were obtained. From the predicted values, the percentages of the friction resistances to the total pullout resistances are 18% and 16% for zinc-coated and PVC-coated wire mesh, respectively. Consequently, the bearing resistances are 82% and 84% of the total pullout resistance for zinc-coated and PVC-coated hexagonal wires, respectively. The ratios of friction to bearing resistances are 22% and 19% for the zinc-coated and the PVC-coated wire meshes, respectively. The total pullout resistance in the zinc-coated mesh is higher than PVC-coated mesh by approximately 20%. Furthermore, the weathered clay backfill was found to have higher pullout resistance and lower pullout displacement than the silty sand backfill.

INTRODUCTION

For soil reinforcements, two design parameters are necessary, tensile strength and bearing (anchorage) resistance. For relatively low modulus soil reinforcement, the load elongation response may also be required. The test methods and design equations for establishing these design parameter have been investigated by several researchers such as Ingold (1983), McGown et al. (1982), Wongsawanon (1998), Voottipruex et al. (2000).

For the bearing resistance, a most significant factor for analysis and design is the interaction behavior between reinforcements and backfill soils. Jewell et al. (1984) have classified the interaction mechanisms into two types, namely: soil sliding over the reinforcement (direct shear mechanism) and pullout of reinforcement (pullout mechanism). Several researchers have done much works on interaction properties between grid reinforcements and soils such as Peterson and Anderson (1980), Jewell et al. (1984), Palmeira and Milligan (1989), Chai (1992), Bergado et al. (1993), Bergado and Chai (1993), and Bergado et al. (1995, 1996).

1 Professor, School of Civil Engineering, Asian Institute of Technology, P.O. Box 4, Klong Luang, Pathumthani 12120, THAILAND.
2 Instructor, King Mongkut's Institute of Technology North Bangkok, 1518 Piboon Songkram Rd., Bangsue, Bangkok 10800, THAILAND.
3 Geotechnical Laboratory Supervisor, School of Civil Engineering, Asian Institute of Technology, P.O. Box 4, Klong Luang, Pathumthani 12120, THAILAND.
4 Doctoral Candidate, School of Civil Engineering, Asian Institute of Technology, P.O. Box 4, Klong Luang, Pathumthani 12100, THAILAND.
Note: discussion on this paper is open until June 1, 2002.

Only few investigators have done research works on the interaction between hexagonal wire mesh and soils. In AIT, Mir (1996), Kabiling (1997), Teerawattanasuk (1997), Bergado et al. (2001a) and Voottipruex et al. (2000) conducted the tests on its pullout and direct shear resistance and found some significant interaction behavior. Bergado et al. (2000) performed a full scale pullout test and found reliable results of interaction behavior. For the analytical prediction, Bergado et al. (2001b) established the prediction model of pullout resistance and displacement behaviors on silty sand. This paper is concerned with the interaction of hexagonal wire reinforcement with compacted weathered Bangkok clay backfill based on the research work of Asanprakit (2000) under the supervision of the first author.

LABORATORY TEST PROGRAM

In this study, weathered Bangkok clay was used as backfill material that is the same material used in previous study (Voottipruex et al. 2000). This material is taken from the topmost soil layer in the Campus of the Asian Institute of Technology (AIT). The index properties of weathered Bangkok clay have previously been verified by several researches and were adopted for this study (Table 1). To prepare the weathered clay before fill in the pullout box, the weathered clay was cured to its optimum moisture condition based on the standard Proctor compaction. A mechanical compaction machine was used in the compaction program. The density and moisture content after compaction (Table 1) was verified by using the Troxler nuclear gauge densitometer and by sand cone method.

Table 1 Index properties of weathered Bangkok Clay (0.2-1.0 m)

Properties	Plangpongpun (1977)	Haque (1977)	Lellasithorn (1978)	Liew (1979)
Physical Properites				
Colour	grey& reddish	grey	reddish grey	grey
Consistency	sitff	stiff	stiff	stiff
In-situ water content, %	30	34	21	30
Sand, %	8±3	5±1	4	17±2
Silt, %	47±3	46±1	36	48±2
Clay, %	45±3	49±2	60	35±2
Specific Gravity	2.71	2.68	2.71	2.70
Liquid limit, %	66±1	62±1	62	60±1
Plastic limit, %	28±1	27±1	27	24±1
Plastic Index	38±1	35±1	35	35±1
Liquidity Index, %	0.05	0.2	0.17	0.17
Activity of Clays, %	-	0.6	-	-
Standard Compaction Test				
Optimum water content, %	24.7	24.1	24.8	23.8
Optimum dry density, kN/m^3	15.5	15.5	15.5	15.5

The hexagonal wire mesh is made of weaving in hexagonal pattern of single wire. The wires now have two types, one is galvanized while another is also galvanized but with PVC sleeved. Galvanized wire has 3.0 mm. diameter and for PVC type has 3.8 mm. diameter. Twisted wires are the longitudinal part of hexagonal wire link. Basically, it is possible to conduct the pullout test for friction resistance of this part by using pre-twisted wires, which are similar to the actual wire mesh. A typical configuration of the PVC-coated wire mesh specimen before pullout test is shown in Fig. 1. Furthermore, pullout tests using seven single wires and similar pullout tests using seven twisted wires each 1.1 m long were done with normal pressures ranging from 35 kPa to 90 kPa (Fig. 2). To consider the bearing behavior, the transverse wires were established. The test program was preformed to evaluate the actual bearing resistance versus displacement and to verify some relevant parameters. Both of two

types of specimens were prepared by shaping a single wire similar to the actual configuration of a transverse wire in a hexagonal wire mesh. The engineering properties and core sizes of both types are the same to the transverse members in hexagonal wire mesh. Pullout tests of transverse wires were designed to observe the mobilized bearing force as shown in Fig. 3. The pullout tests of triple hexagonal cells were performed to observe their displacements and deformations during pullout (Fig. 4).

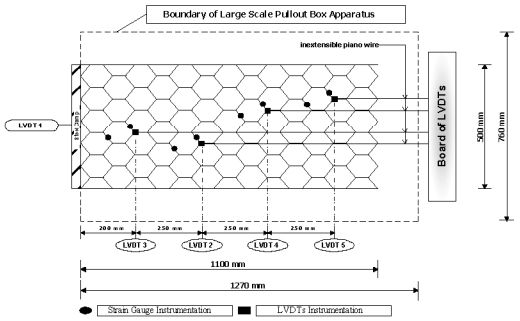

Fig. 1 Sketch of PVC-coated wire mesh sample before testing

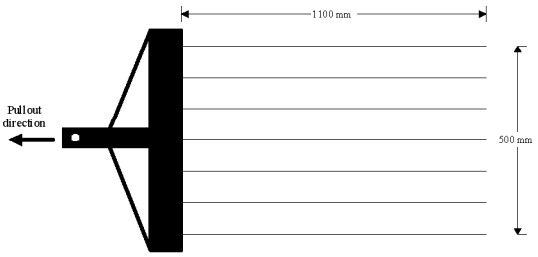

Fig. 2 Seven single/twisted specimens for both zinc-coated and PVC-coated types

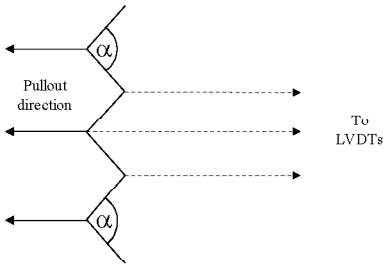

Fig. 3 Typical configuration of transverse wire specimen for pullout test of both galvanized and PVC-coated types

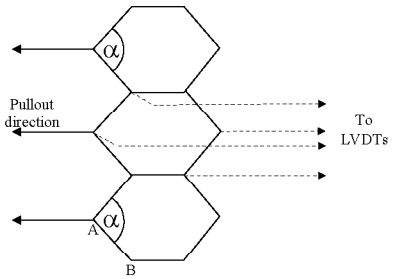

Fig. 4 Typical configuration of triple hexagonal cells specimen for pullout test of both galvanized and PVC-coated types

Table 2 Summary of pullout test programs

List of Test	No. of Test	Normal stress (kPa)	Measurements	Evaluations
Single wire pullout test	8	30, 50, 70, 90	Pullout load and displacement during loading	Friction parameters of single wire in hexagonal wire mesh
Twisted wire pullout test	8	30, 50, 70, 90	Pullout load and displacement during loading	Friction parameters of twisted wire in hexagonal wire mesh
Transverse wire pullout test	8	30, 50, 70, 90	Pullout load and displacement of transverse member	Bearing resistance of transverse member
Triple cell pullout test	8	30, 50, 70, 90	Pullout load and displacement of each member in the cells and its rotation	Behavior during loading and deformation characteristic

Four types of pullout test programs in this study were designed for investigating the pullout resistance mobilization process, the bearing member interaction with weathered clay

as backfill material and the deformation characteristic of each hexagonal cell. Each type of the test program consists of 2 sets of reinforcements (galvanized coated and PVC-coated), each set has 4 tests with 8 tests per type of testing. Four normal pressures consisting of 30, 50, 70, 90 kPa, were applied corresponding to each test. Table 2 tabulates the summary of the pullout test programs.

ANALYTICAL MODELING

General Aspects

The behavior of hexagonal wire mesh reinforcement is complicated due to the deformation of its hexagonal shape which comprises both the deformation and the movement of hexagonal cells. The deformation and movement known as necking phenomena occurred simultaneously during pullout tests. The deformation and movement of the hexagonal cell can be classified into, namely: deformation and translational movement of hexagonal cells in the reinforcement. When the hexagonal cell moves or deforms, the surrounding soil resists through bearing and friction resistances. The bearing resistances are mobilized from three components, namely: deformation of hexagonal cell, translational movement of hexagonal cell in pull direction, and translational movement of hexagonal cell in the lateral direction. In the pullout mechanism, not only pullout resistance is mobilized in the pull direction but also bearing resistance in the lateral direction perpendicular to the pull direction. The bearing resistance due to lateral movement of cell occurred symmetrically with respect to the centerline of the reinforcement in opposite directions and, thus, cancel each other. Therefore, only the pullout resistance from soil bearing resistance in pull direction was accounted for to simplify the model.

At the centerline, the hexagonal cell in the reinforcement has pattern of movement and deformation as shown in Fig. 5. However, the hexagonal cells at the edges moved in both lateral and pull directions (Fig. 6). The total displacement at a node in front of hexagonal cell equals to summation of displacement due to the cell deformation and displacement due to the translational movement of hexagonal cell. During pullout, a lateral bearing resistance perpendicular to the pullout direction was produced but was assumed to be cancelled by a similar resistance of a symmetrically opposite member. The movements and deformations in the pull direction were resisted by the bearing resistance mobilized by orthogonal elements. In the analysis, assumptions were needed to analyze interaction between the reinforcement and backfill soil. Most assumptions were based on the real behavior of hexagonal wire mesh pulled through the backfill soil. Thus, many assumptions were made to determine the interaction between the hexagonal wire mesh and the backfill soil as follows:

1. Deformation of reinforcement is only derived from the rotation of the orthogonal wires.
2. Neglect softening behavior during pullout.
3. Elongation of hexagonal wire mesh reinforcement when embedded in backfill soil corresponds to the effective embedment length and its actual axial stiffness.
4. Neglect the effect of restraint at the front of pullout box.
5. Friction resistance corresponds to linear elastic-perfectly plastic model.
6. Bearing resistance corresponds to hyperbolic model.
7. Fill materials are fully contained in each cell aperture.
8. No bending occurs in the bearing members.
9. The rotational angles and displacements of single orthogonal members during pullout are equal in each row.
10. The bearing resistance in the direction normal to the pullout direction was ignored.

11. Strains in isolated wires are very small when compared to the displacement in the pullout direction and was neglected in the prediction of pullout resistance.

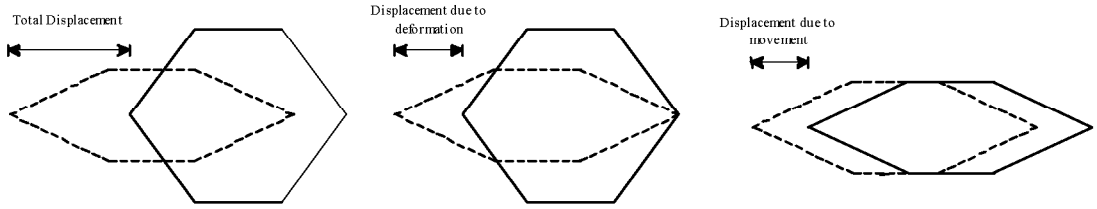

(a) Total displacement (b) Displacement due to deformation (c) Displacement due to movement

Fig. 5 Displacement of single hexagonal cell at centerline of the reinforcement

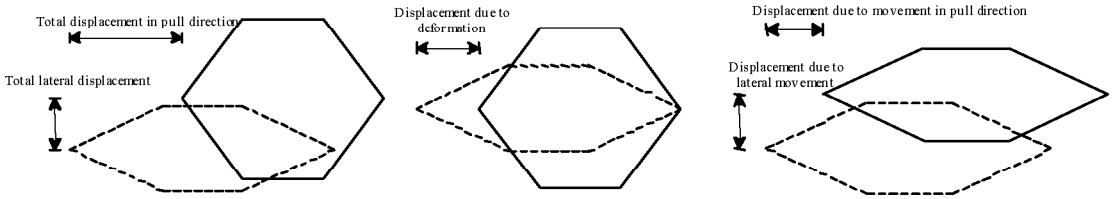

(a) Total displacement (b) Displacement due to deformation (c) Displacement due to movement

Fig. 6 Displacement of single hexagonal cell at edge of the reinforcement

Influence of Transverse Wire Rotation to Displacement of Hexagonal Wire Mesh

During the pullout of hexagonal wire mesh in weathered clay, it was found that the pullout displacement is developed by the movement and rotation or deformation of hexagonal cells. The rotation of transverse wires mainly creates displacements in the pullout direction of hexagonal wire mesh. The proposed analytical model was based on deformation characteristic of the hexagonal cells which can be observed from the actual specimens (Wongsawanon 1998; Srikongsri 1999; Voottipruex 2000). As shown in Fig. 7, the deformation demonstrates two types of displacement. Firstly, the displacement mobilized by transverse wire movement, U_m. Secondly, the displacement mobilized by wire rotation, U_d. Therefore, the relationship of transverse wire movement, wire rotation and total displacement, U_t, during the hexagonal wire mesh reinforcement subjected to applied pullout force can be simulated as Eq. (1):

$$U_t = U_m + U_d \qquad (1), \qquad U_m = L \cot \beta \, (\sin\alpha/2 - \sin(\alpha/2-\theta)) \qquad (2)$$

Consider the nodes at the front and rear of an isolated single transverse wire during the pullout of the reinforcement, a front node (A) is moving toward the pullout direction with the rear node (B) all the time moving on a line inclined from the pullout direction. Due to this movement, the relationship can be extended to describe how the bearing resistance can be mobilized by either total movement or wire rotation. The displacement relationship of the elements in the hexagonal cell has been previously expressed (Wongsawanon 1998).

The analytical approach of this paper improved further the previous concepts by relating the nodal movement of the hexagonal cell to the angle of rotation of a single transverse wire.

Referring to Fig. 7, node B of a single transverse member is moving to the inclined direction and mobilizing the displacement at A. The movement path of B to B' is inclined to the center of reinforcement by the effect of necking phenomena in hexagonal wire mesh. Therefore, the displacement mobilized by movement, U_m, can be expressed in terms of rotational angle of single transverse member as Eq. (2). In Eq. (2), U_m is displacement due to wire movement; L is length of transverse element; α is initial angle of transverse element; θ is rotational angle of a single transverse member and β is angle of nodal movement of single transverse member inclined from pullout direction to the center of reinforcement.

The displacement mobilized by the transverse element rotation or deformation in each row, U_d, can be geometrically related to the rotational angle of the single transverse member. Hence, this relationship can be written as Eq. (3), in which U_d is displacement due to deformation; L is length of transverse element; α is initial angle of transverse element and θ is angle of rotation of isolated single transverse member.

$$U_d = L.(\cos(\alpha/2-\theta)-\cos\alpha/2) \quad (3), \qquad U_t = P_r L_e / EA \quad (4)$$

As shown in Fig. 7, the β-angle may not be constant because the deformed reinforcement may have differences in the cell shapes and sizes corresponding to different types of hexagonal wire specimens. Moreover, the different stiffness of the individual wires of the reinforcement and manufacturing qualities may contribute more complication. However, the β-angle can be determined using the reinforcement axial stiffness obtained from in-air tensile test which also indicated the necking effect. Based on in-air deformation versus tensile force relationship of hexagonal wire mesh reinforcement, the effective embedment length (the length of reinforcement in tension) would correspond to the applied pullout force and its axial stiffness, when subjected to the applied pullout force. The resistance of the surrounding soil is mobilized by the relative movement created from the pullout force. If the resistance corresponding to the displacements along the reinforcement can be computed and the displacements along reinforcement agreed to the proposed displacement relationship, then the effective embedment length and total pullout displacement at the front face can also be determined.

During the pullout of the hexagonal wire mesh reinforcement, the pullout force is resisted by the transverse members and longitudinal members (twisted wires). The magnitude of rotation of transverse members is different in each row. The mobilization of the resistance for each member along the reinforcement varies and in most cases, during pullout process, only a certain part of the reinforcement moved relative to the backfill soil as shown in Fig. 8. These computed values can be related in terms of the axial stiffness of reinforcement, (EA/L_e), and total interaction resistance, P_r. The total displacement, U_t, can then be written as Eq. (4), in which P_r is total interaction resistance corresponding to the computed effective embedment length; L_e is effective embedment length; E is modulus of elasticity of hexagonal wire mesh and A is net cross sectional area of hexagonal wire mesh.

The displacements along the effective embedment length can be computed by trial assuming an initial value of β-angle with desired small pullout displacement at the front face. The details of the iteration process to compute β angle are demonstrated in next sections and the procedure is illustrated in Fig. 10. Then, the computed pullout force as a total interaction resistance can be calculated. Consequently, the computed axial stiffness can be obtained from Eq. 4. The computed axial stiffness is assumed to be equal to the actual stiffness of reinforcement for solving the β-angle. Thus, the calculation has to be iterated by changing the initial β-angle until the convergence between computed and actual axial stiffness of the

reinforcement is achieved. This concept is valid for low strain individual wires which comprised the deformable hexagonal wire mesh.

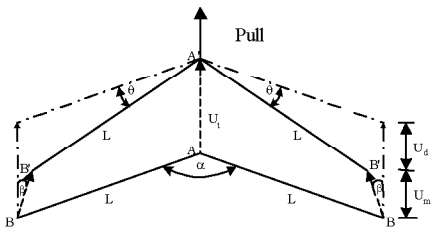

Fig. 7 Deformation characteristic of single transverse wire in hexagonal wire mesh reinforcement

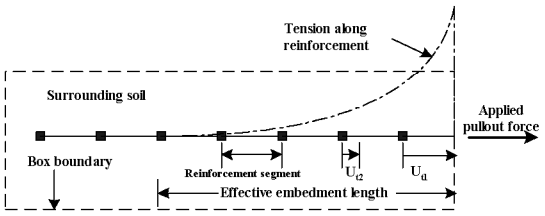

Fig. 8 Movement simulation of the transverse members and the tendency of tension development along its effective embedment length

Deformation Characteristic of Hexagonal Wire Mesh

Referring to an analytical assumption that the displacement of hexagonal wire mesh is mobilized by the rotation of the transverse wires, the strains in the individual wires can be neglected. The total displacement of the hexagonal wire mesh reinforcement, U_t, is equal to the summation of deformation of each transverse wire along the effective embedment length which can be expressed as Eq. (5), in which U_{di} correspond to the nodal displacements due to the hexagonal wire deformations along the effective embedment length with decreasing magnitude away from the pullout face (see in Fig. 8).

$$U_t = \sum_{i=1}^{n} U_{di} \quad (5), \qquad U_{mi} = \sum_{i=(i+1)}^{n} U_{di} \quad (6)$$

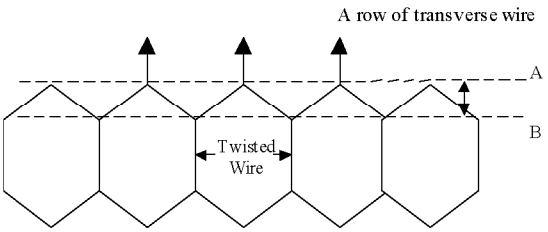

Fig. 9 Illustration of significant parts in hexagonal wire mesh reinforcement

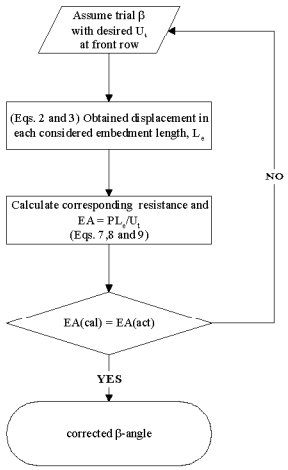

Fig. 10 Flow chart for iteration of the angle of nodal movement inclined from the pullout direction (β) for each considered embedment length, L_e

The amount of movement in each transverse row (Fig. 9) can also be written in terms of the sum of deformations of the successive transverse rows along the effective embedment length. Hence, the movements of transverse wires in the row, U_{mi}, corresponds to the deformations of the transverse wires, U_{di}, and can be obtained as Eq. (6), in which n is the number of rows of deformed transverse wires along its effective embedment length. Equations 5 and 6 can explain how the total displacement and movement of transverse wires in each row are developed by the deformation or rotation of transverse wires along the effective embedment length.

BEARING AND FRICTION RESISTANCES OF HEXAGONAL WIRE MESH REINFORCEMENT

Bearing Resistance

Bergado et al. (2001a) proposed the relationship of bearing force versus displacement of a single hexagonal cell based on hyperbolic model. These expressions were divided into two sources of displacement; one was the bearing resistance due to movement, U_m, and another due to deformation, U_d, as shown in Fig. 7. The bearing resistance of hexagonal wire mesh was considered only in the pullout direction with transverse members. The bearing resistance and displacement relationship proposed by Chai (1992) has been modified by Bergado et al. (2001a) to investigate the mobilized bearing resistance analytically. A new proposed relationship between pullout bearing resistance and displacement was modified from Bergado et al. (2001b). The combination of single transverse wire movement and rotation, the bearing resistance can be expressed as:

$$P_b = L \sin\left(\frac{\alpha}{2} - \theta\right)\left[\frac{U_m}{\frac{1}{E_{ip}} + \frac{U_m}{D\,\sigma_{ult}}} + \frac{L \sin\left(\frac{\theta}{2}\right)}{\frac{1}{E_{ip}} + \frac{2L \sin\left(\frac{\theta}{2}\right)}{D\,\sigma_{ult}}}\right] \tag{7}$$

where L is the length of single transverse member; U_m is the displacement due to movement; E_{ip} is the initial slope of pullout bearing resistance curve; D is the diameter of transverse member; and σ_{ult} is the ultimate pullout bearing resistance.

Friction Resistance

For friction resistance, Mir (1996) and Teerawattanasuk (1997) performed the series of large scale direct shear tests with different fill materials that include a series without reinforcement and series with two types of hexagonal wire mesh, galvanized and PVC-coated. Bergado et al. (2001b) assumed that the shear stress on the interface between the reinforcement and fill material as a linear, elastic, perfectly-plastic model. The friction resistance has been calculated using fraction of skin friction assuming average relative displacement.

Generally, the friction resistance can be separated in two parts: the single transverse wire and the twisted wire. Based on the linear elastic, perfectly-plastic relationship, the friction resistance can be calculated by using the skin frictional area (A_s), shear stiffness (k_s), relative

displacement (u_r), and frictional member length. Then, the friction resistance of twisted wires can be simply calculated as Eq. (8).

$$F_s = k_s u_r A_s \quad (8), \qquad F_s = k_s u_r A_s \cos(\alpha/2 - \theta) \quad (9)$$

Another one is the friction resistance on transverse member. The effect of the transverse wire rotation is the most important factor that will be determined. The projection of relative movement in the pullout direction is needed to formulate the relationship between the friction resistance and relative movement. The friction resistance of this part can be determined by Eq. (9) in which k_s is the shear stiffness of interface; A_s is the frictional area of a wire; and u_r is the relative displacement.

A total of 32 pullout tests were conducted with 16 tests on PVC-coated wires and further 16 tests on zinc-coated wires. The hexagonal wire elements used in the pullout test consist of single friction wires, twisted wires, single transverse wires and triple hexagonal cell. For backfill in the pullout test, weathered Bangkok clay was utilized with normal pressures of 30, 50, 70, and 90 kPa.

PULLOUT RESISTANCE OF SINGLE WIRE

Eight pullout tests each with seven-single wires were done with normal pressures ranging from 30 to 90 kPa. Four were PVC-coated wires and another four were zinc-coated wires. Each wire has 1.1 m length. The test results were plotted in the form of load displacement curves and were normalized into the force per unit length as typically shown in Fig. 11. The zinc-coated wires have lower skin friction than PVC-coated wires because zinc-coated wires have lower diameter than PVC-coated and, consequently, lesser surface area. Both types of hexagonal wires displayed the shear displacement mobilized to reach the ultimate pullout force at displacement of 3 mm. These plots were similar to the linear elastic-perfectly plastic relationship with displacement for mobilizing the maximum friction resistance equal to 3 mm. Similar results were obtained by Bergado et al. (2001a) using silty sand backfill. Tables 3 and 4 show the interface parameters. Some parameters come from previous studies such as cohesion and friction angle. The other parameters were calculated from this study such as shear stiffness.

PULLOUT OF RESISTANCE OF TWISTED WIRE

Similar to the single wires testing, eight pullout tests each with seven-twisted wires at 1.10 m length were done. The results are typically plotted in Fig. 12. The PVC-coated twisted wires have higher friction force than zinc-coated type because zinc-coated type has bigger in diameter than PVC-coated type. It is shown that the ultimate friction resistance was also achieved at 3 mm shear displacements. The shape of curves can be simplified to be linear elastic-perfectly plastic model with displacement for mobilizing the maximum friction resistance equal to 3 mm.

From these test programs on single and twisted wires, the shear stiffness were obtained and used in the analysis. The difference of the interface shear stiffness between the zinc-coated and PVC-coated wire with various normal pressures for single wire and twisted wire are typically shown in Figs. 13 and 14, respectively. It is shown that the interface shear stiffness of the single zinc-coated wire is higher than the single PVC-coated wire because the surface of the zinc-coated wire is rougher than PVC-coated wire. In addition, for twisted wires, the

shear stiffness of the zinc-coated is also higher than the PVC-coated wire as shown in Fig. 14. However, the shear stiffness values of twisted wires/soil interface of both types are closed to the soil/soil interface determined by Mohr-Coulomb failure criteria because the soil can be deposited into the groove of twisted wire and consequently increase its shear resistance. The shear strength at interface between twisted wires and surrounding soil is only slightly lower than the shear strength of soil to soil. Thus, the friction resistance of the twisted member can be calculated using the interface parameters equal to the strength parameters of the backfill soil.

Table 3 Weathered Bangkok clay parameters for predicting the pullout curves

Properties	Fill Material
Backfill soil type	Weathered Bangkok clay
Degree of compaction, %	95
Failure ratio,R_{fp}	0.87
Cohesion, c (kPa)	50
Friction angle, ϕ (degree)	24

Table 4 Basic parameters used for predicting the pullout curves in weathered clay

Backfill Soil Parameter	Weathered clay	
Cohesion, C (kPa)	50	
Friction angle, ϕ (degree)	24	
Failure ratio, R_{fp}	0.87	
Poisson's ratio	0.25	
Reinforcement parameters	Zinc-coated	PVC-coated
Modulus of Elasticity, E (MPa)	2560	2560
Tensile stiffness of wire mesh, EA (kN)	900	900
Diameter of transverse member, D (m)	0.003	0.0038
Length of single transverse member, L (m)	0.06	0.06
Diameter of twisted member, D_T (m)	0.006	0.0076
Length of twisted member, L_T (m)	0.04	0.04
Initial angle of transverse member, α (degree)	96	96
Interface parameters for friction resistance Shear stiffness, k_s (MPa/m)	Zinc-coated 18.4-24.7	PVC-coated 17.6-20.1
Displacement for maximum skin friction, (mm)	3	3
Skin friction angle, δ (degree)	20	16

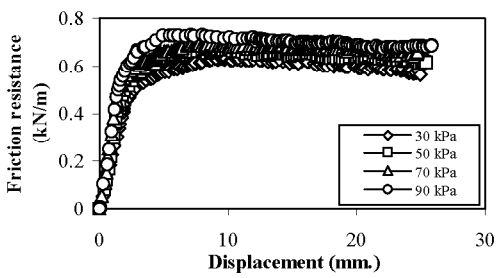

Fig. 11 Friction resistance of PVC-coated wire in weathered Bangkok Clay (single wire)

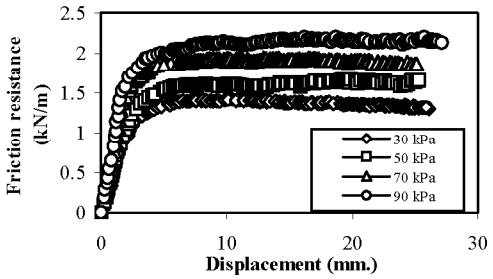

Fig. 12 Friction resistance of PVC-coated wire in weathered Bangkok Clay (twisted wire)

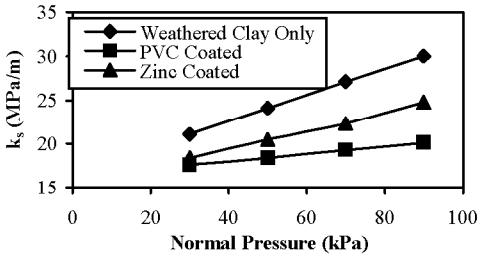

Fig. 13 Shear stiffness of PVC-coated and zinc-coated in weathered Bangkok clay (single wire)

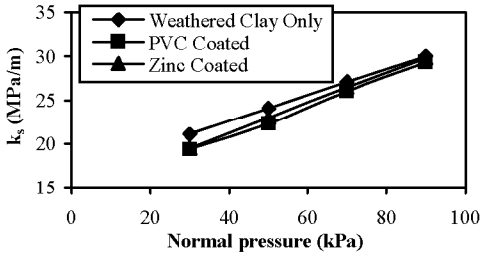

Fig. 14 Shear stiffness of PVC-coated and zinc-coated in weathered Bangkok clay (twisted wire)

PULLOUT RESISTANCE OF SINGLE TRANSVERSE WIRE

This testing program was designed to observe the mobilized bearing force of a single wire during pullout. From the results, the initial slope of pullout bearing resistance curve (E_{ip}) and maximum bearing strength (σ_{bm}) were obtained. The comparison of measured and predicted results by Eq. 7 are typically illustrated in Fig. 15 for zinc-coated hexagonal wire mesh. These curves were normalized to obtain the force per unit width. The force/displacement curves show that progressive force rapidly increased with small displacement. In addition, the curves also show that the test results confirm the predictions very well. Therefore, the bearing resistance of single transverse wire strongly corresponding to the hyperbolic force/displacement relationship and the use of the hyperbolic parameters are reasonable.

For the zinc-coated wire, the ultimate bearing forces were achieved at 3.5, 4.1, 4.7 and 5.2 kN/m corresponding to the applied normal pressures from 30, 50, 70 and 90 kPa. These values agreed with the ultimate bearing force computed by using modified punching shear failure mode (Chai 1992). The computed and measured ultimate bearing forces are tabulated in Table 5 for comparison. For the PVC-coated wire, the ultimate bearing forces were 4.1, 4.5, 5.3 and 6.0 kN/m corresponding to the same applied normal pressures of 30, 50, 70, and 90 kPa. The predictions agreed well with the measured values.

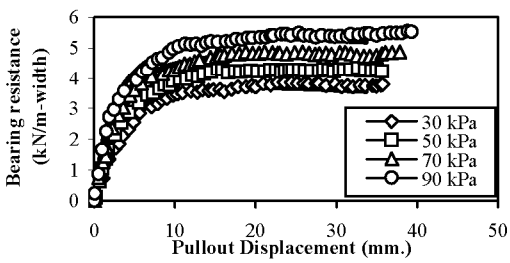

Fig. 15 Mobilized bearing resistance of single transverse zinc-coated wire in weathered Bangkok clay

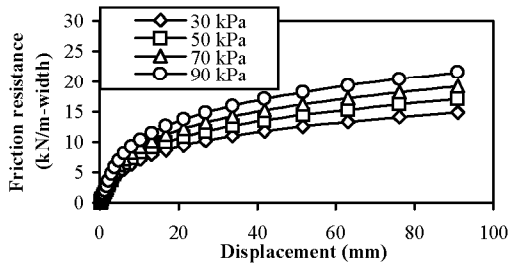

Fig. 16 Predicted friction resistance of zinc-coated wire mesh in weathered Bangkok clay

PREDICTION OF FRICTION RESISTANCE

The predicted total friction resistance was obtained from two sources, namely: from the component in the diagonally-oriented transverse wires and from twisted wires that moved

along the pullout direction relative to the backfill soil. The linear elastic-perfectly plastic model was adopted to simulate the mobilized friction resistance in both hexagonal wire mesh types (Bergado and Chai 1993). The friction force can be computed from Eqs. 8 and 9 corresponding to diagonally-oriented transverse and twisted members based on the interface parameters as listed in Table 4.

In the weathered Bangkok clay backfill, the friction resistance of the PVC-coated and zinc-coated wire with four different normal pressures (30 kPa up to 90 kPa) were predicted. Figure 16 plots the calculated results of the predicted friction resistance from zinc-coated wire mesh. For the zinc-coated wire mesh, the corresponding friction resistance was approximately 18% of total pullout resistance. For the PVC-coated wire mesh, the friction resistance was approximately 16% of total pullout resistance for the range normal pressures. The friction resistance of zinc-coated mesh is slightly more than PVC-coated specimen because the surface texture of the former is rougher than the latter. Furthermore, the PVC sleeve in the PVC-coated wire mesh is smooth geosynthetic material and, thus, the friction force is lower.

PREDICTION OF BEARING RESISTANCE

Figure 17 present the predicted pullout bearing resistances/pullout displacement of zinc-coated wire mesh under various normal pressures in weathered Bangkok clay. These results were computed by using Eq. 7 following the proposed procedures and applying the hyperbolic model. The required parameters were obtained from the laboratory tests listed in Tables 3 and 4. Such parameter as the initial slope of pullout bearing resistance curves, E_{ip}, was obtained by back-calculation from the pullout of single transverse wires. In each normal pressure, the maximum bearing resistances were achieved at pullout displacement of approximately 80 mm for PVC-coated type. However, for the zinc-coated type, it was achieved at shorter pullout displacement of 35 mm corresponding to normal pressure from 30 kPa to 90 kPa. The maximum pullout force was achieved at small displacement because zinc-coated wire mesh has higher stiffness than PVC-coated wire mesh.

The predicted mobilized bearing resistance curves have similar shapes as the total pullout curves. For zinc-coated wire mesh, the bearing resistance was approximately 82% of the total pullout resistance for all normal pressures. While for PVC-coated wire mesh, the bearing resistance was approximately 84% of total pullout resistance. The proportion of bearing resistance of PVC-coated is slightly higher than zinc-coated because the PVC-coated has diameter of 3.80 mm. While the zinc-coated has lower diameter of 3.00 mm. The diameter of wire mesh is important factor for bearing resistance.

PREDICTION OF TOTAL PULLOUT RESISTANCE

In the weathered Bangkok clay backfill, the predicted pullout resistances consisting of bearing and friction resistances of both wire mesh types were combined to obtain the total pullout resistances for different levels of applied normal pressures. These calculated values were validated by comparing to the plots of previous pullout test results (Voottipruex et al. 2000) as illustrated in Fig. 18 for PVC-coated wire meshes and Fig. 19 for zinc-coated wire meshes corresponding to different values of normal pressure. Slight differences were observed because of the limitation of the analytical method and the scatter of test data. However, the predictions agreed with the measured values. Figures 20 and 21 show, respectively, the predicted total pullout resistances of PVC-coated and zinc-coated wire

meshes for all normal pressures. The higher the normal pressure, the higher the total pullout resistance.

COMPARISON OF PULLOUT BEARING AND FRICTION RESISTANCES

Referring to Fig. 20, the highest resistance of PVC-coated wire mesh attained at normal pressure 90 kPa and reduced simultaneously at normal pressures of 70 kPa to 30 kPa. Similarly to the results obtained from the zinc-coated wire mesh, the highest resistance was also attained at normal pressure 90 kPa and reduced simultaneously at normal pressures of 70 kPa to 30 kPa as shown in Fig. 21. Thus, the higher the normal pressure, the higher the total pullout resistance for both types of hexagonal wire meshes. However, the total pullout resistance of zinc-coated hexagonal wire mesh reinforcement is higher than PVC-coated by approximately 20% for the range of normal pressures. From the analytical model, the bearing resistance depended on the initial slope of normalized bearing resistance/displacement curve, E_{ip}. In the weathered Bangkok clay, the E_{ip} values were higher for zinc-coated wire mesh varying from 2250 kPa to 2820 kPa while for PVC-coated wire mesh, the E_{ip} values were lower varying from 2200 kPa to 2440 kpa (Table 5). Moreover, the bearing resistance also depended on diameter of transverse member. The PVC-coated wire has higher bearing resistance in terms of percentage to the total pullout resistance because PVC-coated wire has a bigger diameter. On the other hand, the friction resistance depended on shear stiffness of interface, k_s. In weathered Bangkok clay, the k_s values for zinc-coated wire mesh were higher varying from 18.4 to 24.7 MPa/m while in PVC-coated wire mesh, the k_s values were lower varying from 17.6 to 20.1 MPa/m (Table 4). But, finally, the predicted total pullout resistances consisting of friction and bearing resistances in weathered Bangkok clay can be higher in zinc-coated wire mesh than in PVC-coated wire mesh.

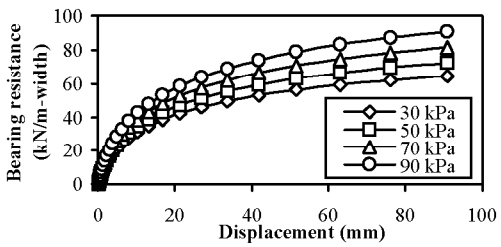

Fig.17 Predicted bearing resistance of zinc-coated wire mesh in weathered Bangkok clay

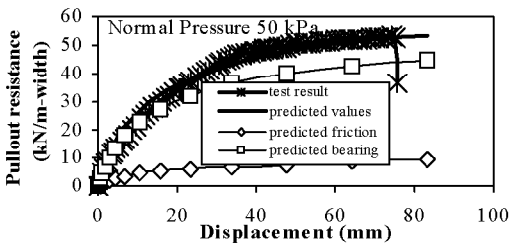

Fig. 18 Predicted pullout resistance of PVC-coated wire mesh in weathered Bangkok clay

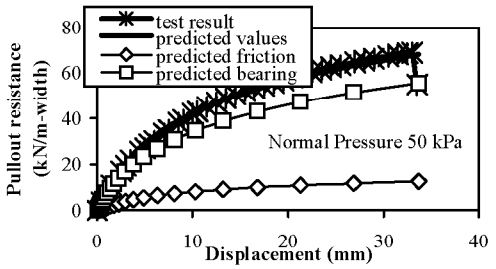

Fig. 19 Predicted pullout resistance of zinc-coated wire mesh in weathered Bangkok clay

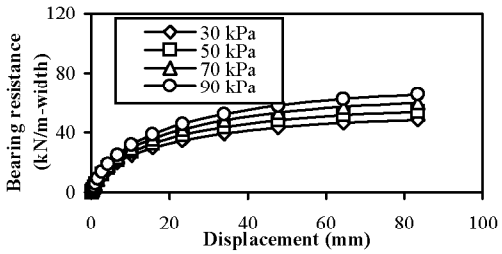

Fig. 20 Predicted total pullout resistance of PVC-coated wire mesh in weathered Bangkok clay

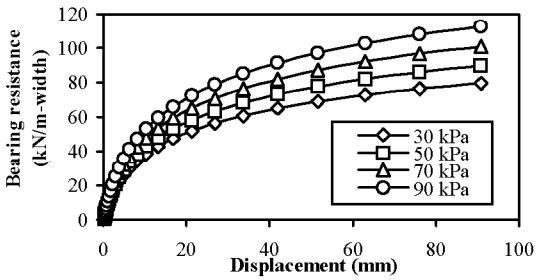

Fig. 21 Predicted total pullout resistance of zinc-coated wire mesh in weathered Bangkok clay

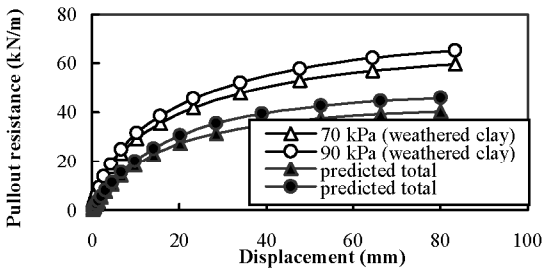

Fig. 22 Comparison of pullout resistance of PVC-coated wire mesh between silty sand and weathered clay backfill

COMPARISON OF PREDICTED PULLOUT RESISTANCES BETWEEN WEATHERED CLAY AND SILTY SAND BACKFILL

The results of the prediction of pullout resistance of PVC-coated hexagonal wire mesh in silty sand (Srikongsri 1999; Bergado et al. 2001b) and weathered Bangkok clay are plotted in Fig. 22. The PVC-coated wire mesh has aperture or cell size of 80 mm x 100 mm. The predicted total pullout resistance in the weathered clay is, on the average, approximately 40% higher than in silty sand. In the weathered clay, the E_{ip} varied from 2200 to 2440 kPa. In silty sand, the E_{ip} values varied from 1000 to 1064 kPa (Srikongsri 1999). In addition, the k_s values ranged from 17.6 to 20.1 MPa/m and 5.5 to 11 MPa/m (Srikongsri 1999) in the weathered clay and silty sand, respectively. Consequently, the predicted pullout resistance developed in the weathered clay can be higher than in the silty sand backfill.

Table 5 Computed parameters used for predicting pullout bearing resistance curves

Parameters		Normal pressure (kPa)			
		30	50	70	90
Ultimate bearing forces (kN/m-width)	Zinc-coated	3.2	3.6	4.3	5.0
	PVC-coated	3.8	4.4	5.0	5.6
Initial slope of pullout curve, E_{ip} (kPa)	Zinc-coated	2250	2380	2600	2820
	PVC-coated	2200	2260	2340	2440

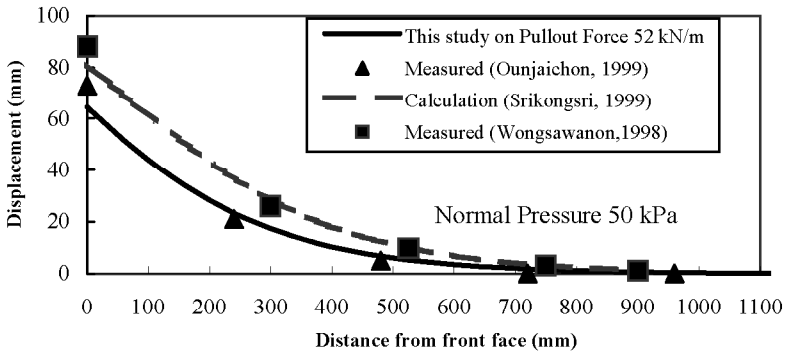

Fig. 23 Comparison on variation of displacement along PVC-coated wire mesh between silty sand and weathered clay

Figure 23 presents the variation of displacements along PVC-coated hexagonal wire mesh on silty sand and weathered Bangkok clay backfills. The measured and predicted of displacements at the front face in silty sand are higher than the corresponding values in weathered Bangkok clay by approximately 10 mm. Thus, the movements in silty sand are higher than in weathered Bangkok clay because the former is weaker than the latter. Therefore, the hexagonal wire mesh yield more elongation in the silty sand backfill than in weathered Bangkok clay.

CONCLUSIONS

An analytical method is proposed to predict the pullout resistance/pullout displacement of hexagonal wire reinforcement. In this method, the friction resistance was simulated by an elastic, perfectly-plastic model while the bearing resistance was simulated by the hyperbolic model. The proposed analytical method can be utilized for predicting the pullout resistance and elongation along reinforcement as well as effective reinforced length. Its validity is confirmed by the reasonable agreement between the predicted and measured pullout resistances. This method can be utilized in weathered Bangkok clay with a maximum of 10% difference between the measured and predicted values.

The total pullout resistance of the hexagonal wire mesh reinforcement is composed of two parts, namely: the bearing and friction resistances. The friction resistances are 18% and 16% of the total pullout resistance for the zinc-coated and the PVC-coated wire meshes, respectively. Consequently, the bearing resistances are 82% and 84% of the total pullout resistance for zinc-coated and PVC-coated hexagonal wires, respectively. The ratios between friction and bearing resistances are 22% and 19% for the zinc-coated and the PVC-coated wire meshes, respectively. The total pullout resistance of zinc-coated hexagonal wire mesh reinforcement is 20% higher than the PVC-coated hexagonal wire. Furthermore, the predicted pullout resistances from the weathered clay backfill were 40 % grater, on the average, than the corresponding values using silty sand backfill. Consequently, the hexagonal wire mesh yielded lower pullout displacements in the weathered clay compared to the silty sand backfill.

REFERENCES

Asanprakit, A. (2000). Analytical model on the distributions of frictional and bearing resistances as well as deformations of hexagonal wire mesh reinforcement with weathered Bangkok clay backfill. M. Eng. Thesis No. GE-99-13. Asian Institute of Technology. Bangkok, Thailand.

Bergado, D. T., Teerawattanasuk, C., Wongsawanon, T. and Voottipruex, P. (2001a). Interaction between hexagonal wire mesh reinforcement and silty sand backfill. Geotechnical Testing Journal. ASTM. 24: 26-41.

Bergado, D. T., Voottipruex, P., Srikongsri, A. and Teerawattanasuk, C. (2001b). Interaction between hexagonal wire mesh reinforcement and silty sand backfill. Canadian Geotechnical Journal. 24: 26-41.

Bergado, D. T., Voottipruex, P., Modmoltin, C. and Kwanpruk, S. (2000). Behavior of a full scale wall test embankment with hexagonal wire mesh. Ground Improvement Journal. 4(2): 47-58.

Bergado, D. T., Chai, J. C. and Miura, N. (1996). Prediction of pullout resistance and pullout force-displacement relationship for inextensible grid reinforcements. Soils and Foundations. 36: 11-12.

Bergado, D. T., Chai, J. C. and Miura, N. (1995). FE analysis of grid reinforced embankment system on soft bangkok clay. Computers and Geotechnics. 17: 447-471.

Bergado, D. T., Shivashankar, R., Alfaro, M. C. and Balasubramaniam, A. S. (1993). Pullout behavior of steel grids reinforcements in a clayey sand. Geotechnique. 43: 589-603.

Bergado, D. T. and Chai, J. C. (1993). Pullout force/displacement relationship of extensible grid reinforcements. Geotextiles and Geomembranes. 13: 295-316.

Chai, J. C. (1992). Interaction behavior between grid reinforcement and cohesive frictional soils and performance of reinforced wall/embankment on soft ground. Doctoral Dissertation No. GT-91-1, Asian Institute of Technology. Bangkok, Thailand.

Haque, M. A. (1997). Some engineering properties of compacted Rangsit clay evaluated on the basis of laboratory tests. M. Eng. Thesis No. 1005, Asian Institute of Technology. Bangkok, Thailand.

Jewell, R. A., Miligan, G. W. E., Sarsby, R. W. and Dubois, D. (1984). Interaction between soil and geogrids. Proc. Of the Symp. On Polymer Grid Reinforcement in Civil Eng, Thomas Telford Limited. London, U.K.: 19-29.

Kabiling, M. B. (1997). Pullout capacity of different hexagonal link wire size and configurations on sandy and volcanic ash (lahar) backfill. M. Eng. Thesis No. GE-96-4, Asian Institute of Technology. Bangkok, Thailand.

Lellasithorn, T. (1978). Strength characteristics of compacted clay. M. Eng. Thesis No. 1286, Asian Institute of Technology. Bangkok, Thailand.

Liew, Y. Y. (1979). Compressibility and permeability characteristics of compacted clay. M. Eng. Thesis No. GT-78-12, Asian Institute of Technology. Bangkok, Thailand.

McGown, A., Andrawes, K. Z. and Kabir, M. H. (1982). Load extension testing of geotextiles confined in soil. Proc. 2nd Intl. Conf. On Geotextiles, Las Vegas. 3: 793-796.

Mir, E. N. (1996). Pullout and direct shear tests of hexagonal wire mesh reinforcements in various fill materials including lahar From Mt. Pinatubo, Phillipines. M. Eng. Thesis No. GE-95-18, Asian Institute of Technology. Bangkok. Thailand.

Ounjaichon, P. (1999). Pullout and direct shear resistance of hexagonal wire mesh reinforcement with weathered Bangkok clay. M. Eng. Thesis No. GT-97-6, Asian Institute of Technology, Bangkok. Thailand.

Palmeira, E. M. and Milligan. G. W. E. (1989). Scale and other factors affecting the results of pullout tests of grids buried in sand. Geotechnique. 39(3): 511-524.

Peterson, L. M. and Anderson, L. R. (1980). Pullout resistance of welded wire mats embedded in Soil. Research Report Submitted to Hilfiker Co., Civil and Environmental Eng. Dept. Utah State Univ. Utah. USA.

Plangpongpun, S. (1977). Strength characteristics of Bangkok clay in relation to pavement design. M. Eng. Thesis No. 1014, Asian Institute of Technology. Bangkok, Thailand.

Srikongsri, A. 1999. Analytical model of interaction between hexagonal wire mesh and silty sand backfill. M.Eng. Thesis No. GE98-17, Asian Institute of Technology. Bangkok, Thailand.

Teerawattanasuk, C. (1997). Interaction and deformation behavior of hexagonal wire mesh reinforcement at vicinity of shear surface on sand and volcanic ash (lahar) backfills. M. Eng. Thesis No. GE-96-14, Asian Institute of Technology. Bangkok, Thailand.

Voottipruex, P., Bergado, D. T. and Ounchaichon, P. (2000). Pullout and direct shear resistance of hexagonal wire mesh reinforcement in weathered Bangkok clay. Geotechnical Engineering Journal of Southeast Asian Geotechnical Society. 31(1): 43.

Wongsawanon, T. (1998). Interaction between hexagonal wire mesh reinforcement and silty sand backfill. M. Eng. Thesis No. GE-97-14, Asian Institute of Technology. Bangkok, Thailand.